T. Adžiev, S. Sedmak†, and B. Petrovski†*

The Effect of Residual Stresses on the Residual Strength of the Welded Pressure Vessel with an Axial Notch

REFERENCE Adžiev, T., Sedmak, S., and Petrovski, B., **The effect of residual stresses on the residual strength of the welded pressure vessel with an axial notch**, *Defect Assessment in Components – Fundamentals and Applications*, ESIS/EGF9 (Edited by J. G. Blauel and K.-H. Schwalbe) 1991, Mechanical Engineering Publications, London, pp. 975–984.

ABSTRACT The paper presents results of an experimental investigation of crack driving force as a measure of residual strength, carried out on two welded pressure vessels. The vessels (1200 mm in diameter, 2600 mm long) are welded of 20 mm thick micro alloyed steel TSt E460. The initial notches (52 × 8.7 mm with the tip radius of 0.05 mm) were produced in heat-affected zone of axial weldments by electrical discharge machine. The vessel 1 was tested in as-welded condition, and the vessel 2 in stress-relieved condition (580°C for two hours).

The residual stresses are measured by the central hole drilling method (ASTM E837) and analysed numerically by the finite element method.

Crack driving forces have been evaluated using the direct measurement of *J* integral. Along the properly selected path 20 strain gauges on the outer side and 11 strain gauges on the inner side were positioned. Crack opening displacement was measured by CMOD gauge.

The final pressure of 162 bar, applied to the vessel 1, produced crack growth of 2.3 mm in depth. The leakage of vessel 2 was achieved by the pressure of 186 bar, with the final crack length of 110 mm. The results of *J* integral direct measurement have been compared with the values, obtained by an elastic–plastic analysis of crack driving force based on Ratwani-Erdogan-Irwin model. The experimental evidence for residual stress and geometrical imperfection effect on residual strength on notched pressure vessel is presented.

Introduction

After one, or few, years of service axial and circumferential cracks were detected in weldments of several cylindrical pressure vessels for liquid gases transportation, made of high strength steels (yield strength over 450 MPa). In some cases cracks have been detected after routine examination of the weldments. Even more serious problems occurred in the spherical storage tanks, made of the same steels, resulting in the leakage of one of them during its exploitation. It is thus natural that the estimation of residual strength of welded pressure vessel with a crack became very important problem in service.

The investigation, carried out so far regarding safety analysis of welded structures, pointed out that besides material and weldment characteristics, the residual stresses play an important role. The residual stresses, induced by welding, have not only the important contribution in crack growth, but they also can help the appearance of cracks, such as hydrogen and lamelar cracks, and other similar defects. Residual stresses are usually relaxed by the heat treatment after welding (HTAW), with an aim to increase the toughness and

* Faculty of Mechanical Engineering, University of Skopje, Yugoslavia.
† Faculty of Technology and Metallurgy, University of Belgrade, Yugoslavia.

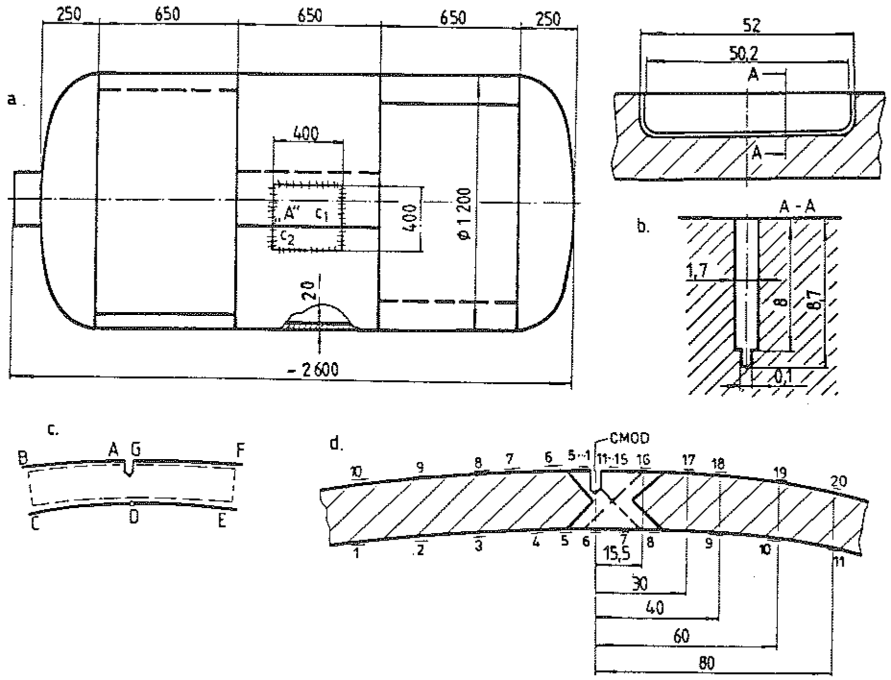

Fig 1 **Experimental pressure vessel: (a) shape and dimension, (b) crack cross-section, (c) *J* integral contour, (d) strain gauges distribution around notch**

reduce the risk of brittle fracture. In the case of pressure vessels the HTAW is regulated as a standard procedure. Anyhow, there are at least two problems concerning the application of HTAW: high costs and possible reduction (instead of increase) of the toughness in the case of micro alloyed steels.

Pressure vessel material and production

Two full-scale pressure vessel models (Fig. 1) were produced of micro alloyed T St E460 steel from Steelworks Skopje for the analysis of residual stress influence on crack behaviour. The chemical composition of T St E460 steel is given in Table 1, as an average of several tests. Tensile properties, tested for T St E460 steel after normalisation at 900°C and after heat treatment for stress relieving (580°C for two hours) are listed in Table 2.

In order to avoid an exaggerated overmatching effect, EPP2 wire and OP40TT flux from Steelworks Jesenice were applied for submerged-arc-welding (SAW) of pressure vessels. Welding has been performed in four layers

Table 1 **Chemical composition of T St E460 steel**

C	*Si*	*Mn*	*P*	*S*	*Cu*	*Ni*	*Cr*	*V*	*Nb*	*Al*
0.105	0.265	1.63	0.022	0.017	0.22	0.58	0.12	0.105	0.027	0.041

Table 2 **Tensile properties of T St E460 steel**

Heat treatment	*Yield strength* R_e *(MPa)*	*Ultimate tensile strength* R_m *(MPa)*	*Elongation* A_5 *(%)*
Normalisation at 900°C	445	645	24
Stress relieving at 580°C for 2 h after normalisation	460	625	24.5

Table 3 **Chemical composition and mechanical properties of weld metal deposit (EPP2 Wire and OP40TT Flux)**

Chemical composition			*Yield strength* R_e *(MPa)*	*Ultimate tensile strength* R_m *(MPa)*	*Elongation* A_5 *(%)*	*Charpy 'V' impact Energy at −20°C* *E* (J)
C	*Si*	*Mn*				
0.07	0.30	0.90	>390	480–550	>24	>70

Table 4 **Tensile properties of weld metal, obtained in T St E460 steel by submerged-arc-welding with EPP2 wire and OP40TT flux**

Yield strength R_e *(MPa)*	*Ultimate tensile strength* R_m *(MPa)*	*Elongation* A_5 *(%)*
482	669	18.5

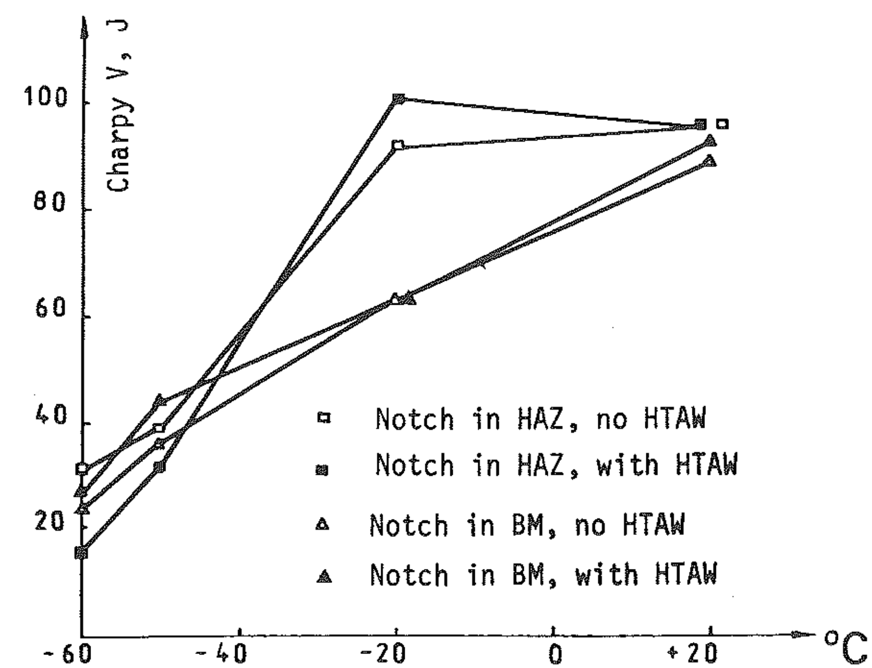

Fig 2 **Charpy notch toughness in the base metal and heat affected zone**

with heat input 1.5–1.8 MJ/m. Chemical composition and mechanical properties of weld metal deposit, specified by Steelworks Jesenice, are given in Table 3. Tensile properties of weld metal are determined on specimens, taken from trial samples, welded under the same conditions and in the same time as pressure vessel without HTAW. Typical results are given in Table 4.

The overmatching effect was not too extreme, as one can conclude comparing the results given in Table 2 and Table 4.

The first pressure vessel (marked as vessel 1) has been tested in as-welded condition. The second pressure vessel (marked as vessel 2) was heat treated at 580°C for 2 hours after welding for stress relieving before testing.

Impact toughness examination of heat treated samples

Charpy 'V' toughness examination, performed according to ISO standard, was carried out in order to distinguish the residual stresses effects from an eventual effect of the HTAW. The effect of HTAW on structural changes and mechanical properties of a weldment can be significant. Charpy 'V' specimens are typically free of residual stresses because of their small sizes and for this reason they can be used for estimation of HTAW effect on material toughness.

The results of toughness examination, carried out for two different series of specimens (with and without HTAW) are shown in Fig. 2. As it can be seen, there is hardly any influence of the HTAW on the Charpy 'V' impact toughness in the base metal and heat affected zone (HAZ).

Residual stresses

Residual stresses were experimentally evaluated around the part of axial weldment, positioned on the sample indicated by 'A' in Fig. 1(a), welded on the middle ring of a mantle. The measurement has been performed by central hole drilling method **(1)** using RS-200 equipment (Measurement Group Inc, USA) and strain gauges RY-61 (HBM, FRG). The disposition of some strain gauges is presented in Fig. 3. Residual stress measurement was performed before (Fig. 3(a)) and after (Fig. 3(b)) preparing of notches C1 and C2 (compare also Fig. 1). The results of residual stress measurement are presented in Fig. 4(a) for vessel

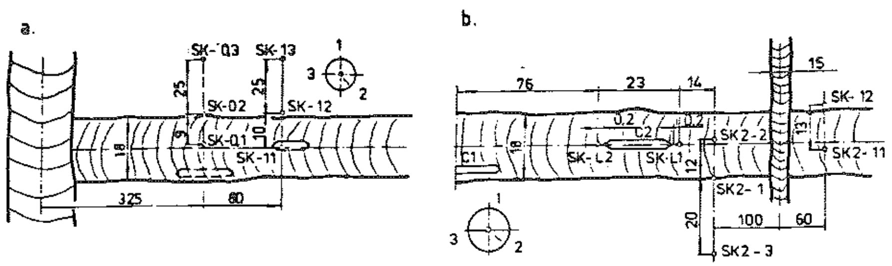

Fig 3 Strain gauges disposition in the notched region on sample 'A' for residual stress measurement, (a) before and (b) after notch machining

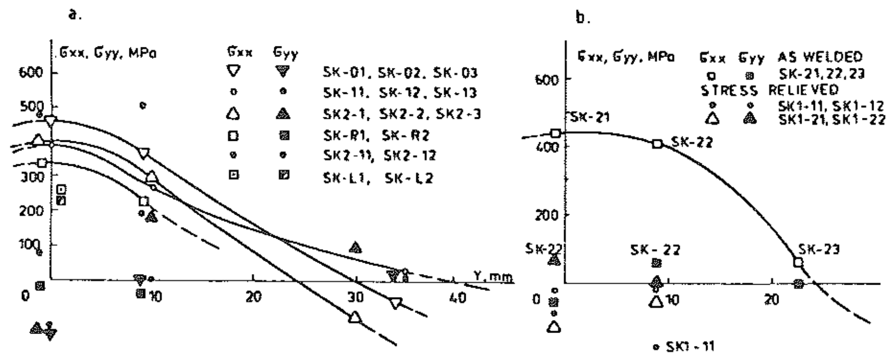

Fig 4 Residual stress components σ_{xx} and σ_{yy} experimentally measured on: (a) pressure vessel 1 in as-welded condition, and (b) on pressure vessel 2 before and after stress relieving

1 and in Fig. 4(b) for vessel 2 before (in as-welded condition) and after stress relieving by heat treatment. The magnitudes of residual stresses, measured in stress-relieved condition after HTAW, indicated high degree of stress relaxation.

Additional numerical analysis of residual stresses has been performed by finite elements method **(2)**. Results obtained in this analysis for different heat inputs Q and material yield strengths R_e are presented in Fig. 5 **(3)**.

Comparing experimental and numerical results for the vessel 1, one can see good agreement for σ_{xx} component of residual stresses with an overall level close to the yield strength (Fig. 4(a), Fig. 5). On the other hand, in the case of σ_{yy} component the agreement was not so good, since the experiment indicated

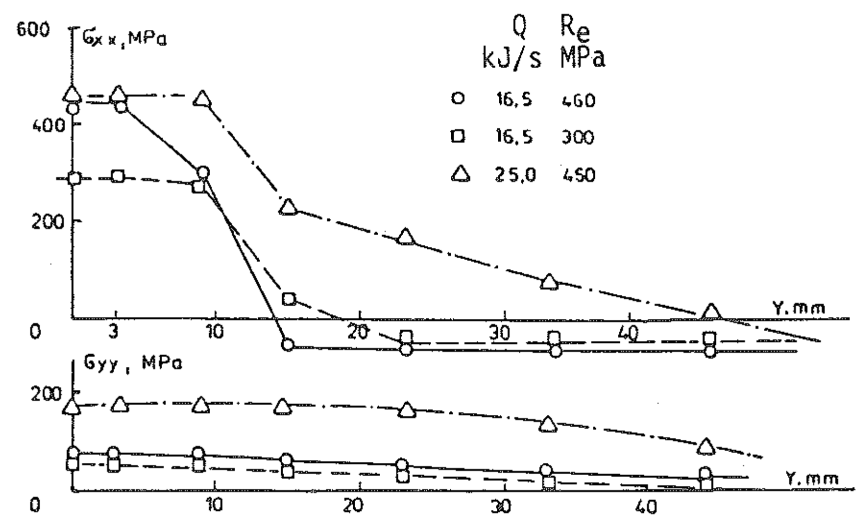

Fig 5 Numerically determined residual stress components σ_{xx} and σ_{yy} for different heat inputs Q and different yield strength levels R_e

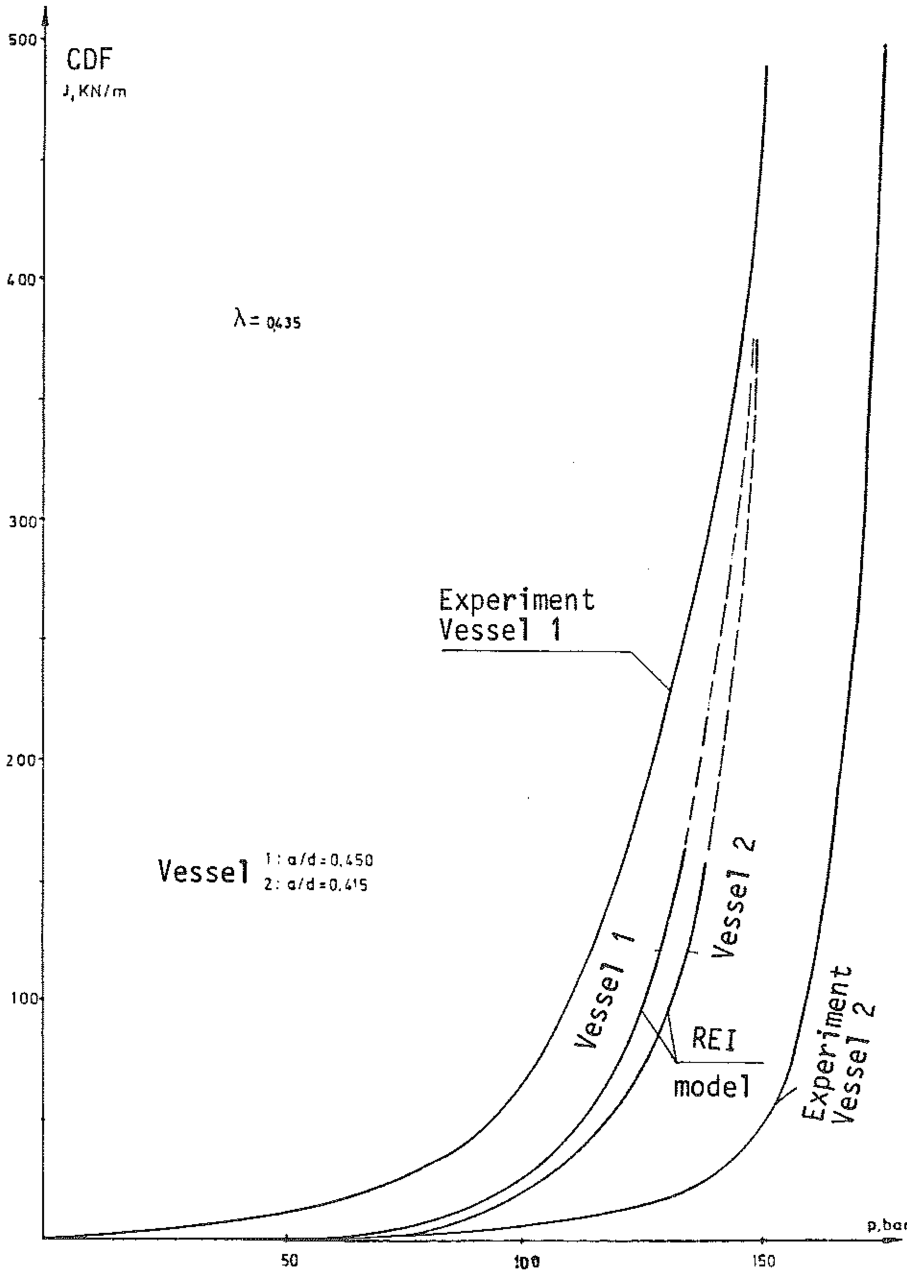

Fig 6 Crack driving force expressed by *J* integral versus pressure

higher values (40 percent of yield strength) compared to the results of numerical analysis. Having this in mind, as well as some unexpected experimental results (compressive σ_{yy} stresses in some measuring points) it has been concluded that 20 percent of yield strength corresponds to σ_{yy} component of the residual stresses, according to numerical analysis **(4)**.

Crack driving force evaluation

Using Barenblatt-Dugdale model of plastic zone around the crack tip Ratwani *et al.* **(5)** have expressed *J* integral for thin cylindrical shell with an axial part-through crack (REI model, see Fig. 6), as follows

$$J = \frac{8}{\sqrt{3}} \frac{c\sigma_Y}{E} \left\{ \frac{\delta_0}{d_1} + \frac{\theta_2}{d_2}\left(0.5 - \frac{a}{w}\right) \right\} \tag{1}$$

where $d_1 = 4c\sigma_Y/E$ and $d_2 = 4c\sigma_Y/wE$, $2c$ denotes crack length, a crack depth, E modulus of elasticity (210 GPa), v Poisson's ratio (0.3), σ_Y yield strength (482 MPa – see Table 4), w wall thickness (20 mm, δ_0 crack opening displacement, and θ_2 distortion angle. The ratios δ_0/d_1 and θ_2/d_2 are given in **(5)** as a function of applied pressure p and λ, shell parameter defined in the form

$$\lambda = \{12(1 - v^2)\}^{1/4} \frac{c}{\sqrt{Rw}} \tag{2}$$

Here, R stands for shell radius (590 mm). Using relation (1) it is possible to plot crack driving forces (CDF), expressed by J versus p for both vessels (Fig. 6). Differences in curves are the consequence of different crack depths, measured after breaking of ligaments.

Direct measurement of J integral **(6)** was carried out on both vessels (Fig. 1). Cracks were made by electrical discharge machine with tips positioned in HAZ (Fig. 1(b) and 1(d)). J integral contour was instrumented by 31 strain gauges, 20 on the outer and 11 on the inner vessel surface (Fig. 1(d)), and CMOD measuring device was applied.

For the contour ABCDEFG (Fig. 1(c)) J integral is expressed as

$$J = SW^{i}_{cr} + SW^{0}_{cr} - ST \tag{3}$$

where SW^{i}_{cr} and SW^{0}_{cr} denote the strain energy density on inner and outer surface, respectively, and ST is the tension–bending term contribution. The results of CDF evaluated by J integral direct measurements are also presented in Fig. 6, as the plot J versus p for both vessel 1 and vessel 2.

Discussion

According to the results, obtained for crack driving forces in the form of J integral in the experiment with two different vessesl, residual stresses relaxation by heat treatment is beneficial for the crack growth resistance and fracture safety in these welded structures. However, crack growth behaviour in a real structure is depended not only on residual stresses and their relaxation, but also on the other effects. The performed experiments enabled only the overall crack behaviour evaluation, from which the individual effects have to be separated. Some metallurgical effects can reduce toughness properties, especially in the HAZ of micro-alloyed steels. If the zone of reduced toughness is relatively small there is a good chance for crack not to grow. On the contrary, if the zone is large (more than few millimetres) this has to be taken into account when residual strength and fracture safety are estimated. Having this in mind, such an analysis is made here, with the results that there are no damaging metallurgical effects on toughness in HAZ (Fig. 2). Anyhow, this estimation should be done on a more complex basis, concerning also temperature and time period of the relieving process.

The second important influence on the crack growth resistance can be attributed to the weldment geometry. Generally, vessel geometry depends on deviations from the cylindrical shape, primarily due to misalignment of plate edges and angular distortion, influencing also weldment geometry and consequently the magnitude and distribution of residual stresses. These geometry imperfections are also important during loading because they can cause additional forces and moments. Anyhow, this additional load is not necessarily damaging, because it can act toward a reduction of crack driving force. Geometry effect was observed during the examination of the vessel 2. As it is shown in Fig. 7, there is a deviation from the cylindrical shape in the region of weldment, what is primarily the consequence of poor forming of plates edges. Results for J versus p (Fig. 6) and an analysis of local behaviour of crack tip surroundings (Fig. 8(a), (b)) indicate a beneficial effect of the irregular geometry, obviously due to the additional bending moment acting in the opposite direction to the pressure in the case of vessel 2. This practically means that, depending on the fabrication processes (bending and welding), the local region around an axial weldment can be of ideally cylindrical shape or either convex or concave compared to it. It could be speculated that a geometry misalignment different to the one shown in Fig. 7 would cause a damaging effect, increasing the crack driving force. It should be also mentioned that the vessel 1 did not have any effect of geometry in the aofrementioned sense.

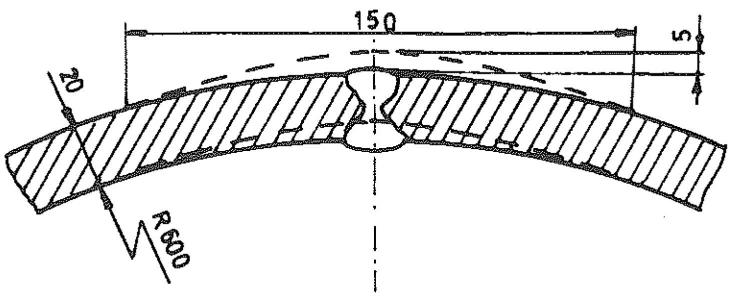

Fig 7 Weldment geometry – pressure vessel 2

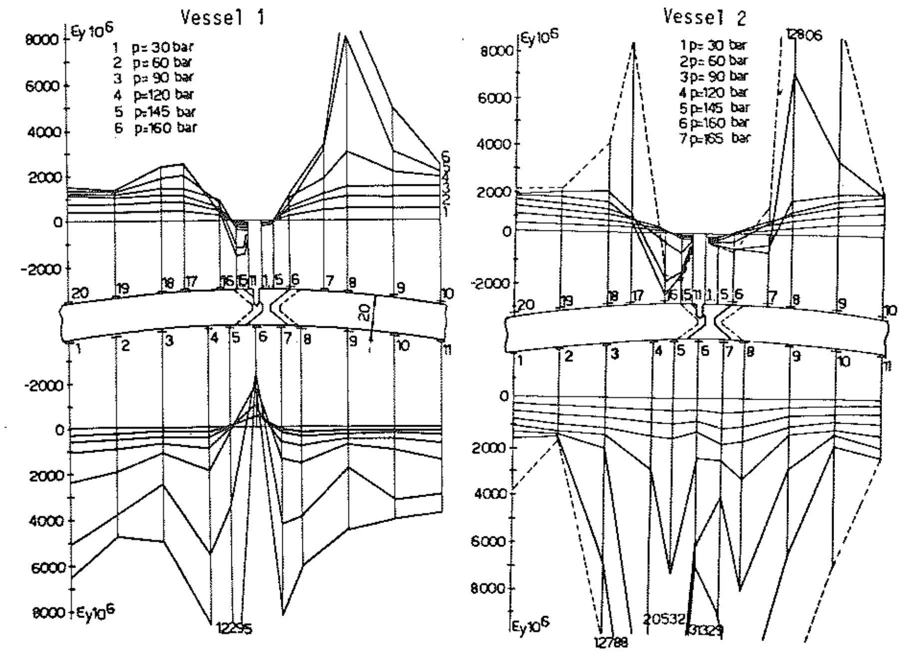

Fig 8 The distribution of ε_{yy} strain component along J integral path on notched and smooth sides

The experimental procedure for the vessel 1 was interrupted before fracturing with crack advance in depth for 2.3 mm at the pressure level of 162 bar. Pressure level of 182 bar caused leakage of vessel 2 with the final crack length of 110 mm, indicating the stable manner of crack growth. Anyhow, the stable crack growth in both vessels was possible only after local plastic deformation and the appropriate redistribution of residual stresses. The effect of local plastification on the redistribution of residual stresses needs further investigations.

By comparing the CDF curves one can conclude that REI model gives a conservative estimate of the residual strength of vessel 2. It is clear that geometry imperfections have contributed to this effect, since residual stresses have been relaxed. On the contrary, REI model predicted lower CDF curves, compared to the experimental results, in the case of vessel 1 where the residual stresses had not been relieved. Therefore, if a conservative model is to be applied, the REI model should be corrected in this case.

The failure criterion expressed through J integral should include residual stresses in the case of welded structure without HTAW. Geometrical imperfection is another influencing factor which has to be taken into account, so that the failure criterion could expressed as follows

$$J_{Ic}^{real} = J_{Ic} + J^{rs} + J^{g} \qquad (4)$$

where J^{rs} corresponds to the residual stresses effect and J^{g} to the influence of geometrical shape. For vessel 2, term J^{g} contributed to increase of service safety, and term J^{rs} could be neglected according to the level of σ_{yy} component values for stress relieved pressure vessel (Fig. 4(b)). For the vessel 1, geometrical effect could be neglected because of cylindrical shape ($J^{g} \cong 0$) and the J^{rs} value decreases the pressure vessel safety, because of definitive σ_{yy} component value in tension.

One should also be aware of the biaxial stress state in the pressure vessel and its possible influence on the crack driving force. Since there is not enough evidence of this influence, one can only make a general statement that the additional investigations are needed in order to separate effects described here and any other possible effect not taken into account so far. Toward this end small specimens and tensile panels will be tested soon.

Conclusions

A method of J integral direct evaluation, applied in full-scale pressure vessel test on notched models for crack driving force evaluation in as-welded and stress-relieved conditions, provided experimental evidence of the residual stress effect on residual strength, and of the beneficial effect of heat treatment after welding on the crack driving force and crack behaviour. Further investigations are required for separation of individual effects of residual stresses and geometrical imperfections on crack driving force in a real pressure vessel.

References

(1) ASTM E837-85 (1988) Standard test method for determining residual stress by the hole-drilling strain-gauge method, *Annual Book of ASTM Standards,* ASTM, Philadelphia.
(2) HIBBIT, H. D. (1972) *A numerical thermo-mechanical model for the welding and subsequent loading of a fabricated structure*, PhD Thesis, Brown University, RI.
(3) ADZIEV, T. (1988) *Contribution to investigation of an influence of residual stresses to the crack resistance of welded structure,* (in Macedonian) PhD Thesis, University of Skopje, Yugoslavia.
(4) ADZIEV, T. *et al.* (1988) Residual stresses and their effect on J integral behaviour in full-scale pressure vessel test, ICRS2, Nancy.
(5) RATWANI, M., ERDOGAN, F., and IRWIN, G. (1974) Fracture propagation in a cylindrical shell containing an initial flaw, Lehigh University, Bethlehem, PA.
(6) READ, D. T. (1983) Experimental method for direct evaluation of the J contour integral, *ASTM STP 791*, ASTM, Philadelphia, pp. 11–199.